

# Accepted Manuscript

The SEVAN Worldwide network of particle detectors: 10 years of operation

A. Chilingarian, V. Babayan, T. Karapetyan, B. Mailyan, B. Sargsyan, M. Zazyan

PII: S0273-1177(18)30172-8

DOI: <https://doi.org/10.1016/j.asr.2018.02.030>

Reference: JASR 13648

To appear in: *Advances in Space Research*

Received Date: 9 June 2017

Revised Date: 23 February 2018

Accepted Date: 24 February 2018



Please cite this article as: Chilingarian, A., Babayan, V., Karapetyan, T., Mailyan, B., Sargsyan, B., Zazyan, M., The SEVAN Worldwide network of particle detectors: 10 years of operation, *Advances in Space Research* (2018), doi: <https://doi.org/10.1016/j.asr.2018.02.030>

This is a PDF file of an unedited manuscript that has been accepted for publication. As a service to our customers we are providing this early version of the manuscript. The manuscript will undergo copyediting, typesetting, and review of the resulting proof before it is published in its final form. Please note that during the production process errors may be discovered which could affect the content, and all legal disclaimers that apply to the journal pertain.

# The SEVAN Worldwide network of particle detectors: 10 years of operation

**A. Chilingarian<sup>1,2,3</sup>, V. Babayan<sup>1</sup>, T. Karapetyan<sup>1</sup>, B. Mailyan<sup>4</sup>, B. Sargsyan<sup>1</sup>, and M. Zazyan<sup>1</sup>**

**<sup>1</sup>A. Alikhanyan National Lab (Yerevan Physics Institute), 2 Alikhanyan Brothers, Yerevan 0036, Armenia**

**<sup>2</sup>National Research Nuclear University MEPhI (Moscow Engineering Physics Institute), Moscow 115409, Russian Federation**

**<sup>3</sup>Space Research Institute of RAS, Moscow, Russia**

**<sup>4</sup>Department of Physics and Space Sciences, Florida Institute of Technology, FL, USA**

**Key words:** cosmic rays, networks of particle detectors

## Abstract

The Space Environment Viewing and Analysis Network (SEVAN) aims to improve the fundamental research on particle acceleration in the vicinity of the sun, on space weather effects and on high-energy physics in the atmosphere and lightning initiation. This new type of a particle detector setup simultaneously measures fluxes of most species of secondary cosmic rays, thus being a powerful integrated device for exploration of solar modulation effects and electron acceleration in the thunderstorm atmosphere. The SEVAN modules are operating at the Aragats Space Environmental Center (ASEC) in Armenia, in Croatia, Bulgaria, Slovakia, the Czech Republic (from 2017) and in India. In this paper, we present the most interesting results of the SEVAN network operation during the last decade. We present this review on the occasion of the 10<sup>th</sup> anniversary of the International Heliophysical Year in 2007.

## 1. Introduction

The sun influences earth in different ways by emission of electromagnetic radiation, solar plasmas, and high-energy particles. Although the total energy of the emitted particles comprises a very small fraction of the energy of the visible light, the study of these particles provides valuable information on the huge solar explosions which affect the near-earth space, space-borne and surface technologies, i.e. on the so-called space weather. In 1957, in an unprecedented international cooperation, more than 66.000 scientists and engineers from 67 nations perform measurements of the major geophysical parameters in the framework of the International Geophysical Year (IGY1957, Chapman, 1959). Fifty years on, the International Heliophysical Year (IHY 2007, Thompson et al., 2009) again drew scientists and engineers from around the globe in a coordinated observation campaign of the heliosphere and its effects on planet earth. The United Nations Office for Outer Space Affairs, through the United Nations Basic Space Science Initiative (UNBSSI), assisted scientists and engineers from all over the world in participating in the IHY. The most successful IHY 2007 program was to deploy arrays of small, inexpensive instruments around the world to get global measurements of ionospheric and heliospheric phenomena. The small instrument program was (and still is) a partnership between instrument developers and instrument hosts in developing countries. The lead scientist prepared and installed the instruments and helped to run it; the host countries provided manpower for instrument operation and maintenance. The lead scientist's institution developed joint databases, prepared tools for user-friendly access to the data, assisted in staff training and paper writing to promote space science activities in developing countries.

The sun is a tremendously variable object, capable of changing the fluxes of the Solar Cosmic Rays (SCR) by 3–4 orders of magnitude in a span of a few minutes. These transient events are called “Solar Proton Events (SPEs)” and “Solar Energetic Particle (SEP) events”. Because of the sun's closeness, the effects of the changing fluxes can have a major influence on the earth, including climate, safety, and other areas. The sun “modulates” the low energy Galactic Cosmic Rays (GCR) in several ways. Along with broadband electromagnetic radiation, the explosive flaring processes on the sun usually

result in Coronal Mass Ejections (CME) and in acceleration of copious electrons and ions. Particles can be generated either directly in the coronal flare site with a subsequent escape into interplanetary space, or they can be accelerated in CME-associated shocks that propagate through the corona and interplanetary space. These particles are effectively registered by spectrometers located at the Lagrangian point L1 (SOHO, ACE) and on satellites (GOES, SDO). In recent years, the increasing precision and extended energy range of direct cosmic ray measurements supplied by AMS-02 and PAMELA allow shedding light on the details of the solar modulation during solar cycles 23 and 24 (Corti et al., 2015). However, the small size of satellite-based detectors and the small number of satellites does not provide sufficient statistics in the high-energy region for real-time monitoring of the space weather. Therefore, space and ground observations should be conducted simultaneously in a way to provide complementary information.

Networks of particle detectors on earth, located at different latitudes and altitudes are monitoring the solar activity for many decades without interruptions. The highest energy SCRs generate particle showers in interactions with atmospheric nuclei that can reach the earth surface and generate signals in surface particle detectors (similar to ones initiated by GCRs). Such events are called Ground Level Enhancement (GLE). The latitude dependence of the geomagnetic field provides the possibility to use worldwide networks of Neutron Monitors (NM; Hatton, 1971, Simpson, 2000, Moraal, 2000) as a spectrometer, registering GCR in the energy range from 0.5 to 10 GeV.

The spectra of GCR can be approximated by a power law  $dJ/dE \sim E^{-\gamma}$  with  $\gamma \sim 2.7$ . The intensity of the SEP events at energies above hundreds of MeV usually decay very fast (with exponential cut-off of the power-law spectrum; Miroshnichenko and Nymmik, 2014). Only for some events, such as the one on 20 January 2005, the spectra of SCR are considerably “harder”, reaching energies up to 1 GeV (see Fig. 1 from Labrador et al., 2005 and Tab. 1 in Asvestari et al., 2017). Thus, for the GeV energies the intensity of the GCR becomes increasingly higher than the intensity of the largest observed SEP events and we are confronted with the very complicated problem of detecting a small signal from the sun

against the huge “background” of the GCR. Most existing networks of particle detectors are unable to reliably detect very low particle fluxes of SEP events in the GeV region. Therefore, the maximal energy of solar accelerators is still not determined (Miroshnichenko, 2014). However, measurements at the Aragats Space-Environmental Center (ASEC, Chilingarian, 2005) of the huge SEP of January 2005 with a large underground muon detector allowed an estimate of the maximal energy of solar proton accelerators to be up to 20 GeV and more (Bostanjyan & Chilingarian, 2007, Chilingarian & Bostanjyan, 2009). Through measurements of enhanced secondary fluxes of the various charged and neutral particles at the surface of the earth, it is possible to estimate the power law index of the SEP energy spectra. Considerably large values of the recovered spectral index ( $\gamma = 4 - 5$ ) at GeV energies is a very good indicator for the upcoming severe radiation storm (abundant SCR protons and ions with energies 50 - 100 MeV, see Chilingarian and Reymers, 2007), dangerous for astronauts, high polar airplane flights and satellite electronics. Each of the measured secondary particle fluxes has a different, most-probable energy of the primary “parent” (i.e. proton or nucleus). As we demonstrated in (Zazyan & Chilingarian, 2009), for the Aragats facilities these energies vary from 7 GeV (most probable energy of primary protons creating neutrons) to 20-40 GeV (most probable energy of primary protons generating muons with energies above 5 GeV). Thus, for predicting upcoming radiation storms it is necessary to monitor changing fluxes of the different species of secondary cosmic rays with various energy thresholds. To cover a wide range of secondary cosmic rays energies we need networks of particle detectors at different latitudes longitudes and altitudes.

Other solar modulation effects also influence the intensity of the cosmic rays in the vicinity of the earth. Huge magnetized plasma structures usually headed by shock waves travel into the interplanetary space with velocities up to 3000 km/s (so-called interplanetary coronal mass ejection - ICME) and disturb the interplanetary magnetic field (IMF) and magnetosphere. These disturbances can lead to major geomagnetic storms harming multibillion assets in the space and at ground. At the same time, these disturbances introduce anisotropy in the GCR flux. Thus, time series of intensities of high-energy particles can provide highly cost-effective information also for the forecasting of the geomagnetic

storm (Leerungnavarat et al., 2003). With data from networks of particle detectors, we can estimate the GCR energy range affected by ICME and reveal the energy-dependent pattern of the ICME modulation effects. For instance, surface particle detectors can precisely measure the attenuation of the GCR flux in the course of a few hours with following recovering during several days (Forbush decreases, FD, see Bostanjyan, Chilingarian, 2009). Measurements of the FD magnitude in the fluxes of different secondary CR species reveal important correlations with the speed, size of the ICME and the “frozen” in ICME magnetic field strength (Chilingarian and Bostanjyan, 2010). Measurements of all the secondary cosmic-ray fluxes at one and the same location are preferable due to effects of the longitudinal dependence of the FD magnitudes (Haurwitz et al., 1965). The research of the diurnal variations of GCR by the observed fluxes of charged and neutral secondary CR also opens possibilities to correlate the changes of parameters of the daily wave (amplitude, phase, maximal limiting rigidity) with the energy of GCRs (Mailyan and Chilingarian, 2010).

Thus, for the basic research of solar physics, solar-terrestrial connections and space weather, as well as for establishing services of alerting and forecasting of dangerous consequences of space storm the networks of particle detectors located at different geographical coordinates and measuring various species of secondary cosmic rays are of vital importance.

A network of particle detectors located at middle to low latitudes known as SEVAN (Space Environment Viewing and Analysis Network, Fig. 1, Chilingarian &Reymers, 2008, Chilingarian et al., 2009) was developed in the framework of the International Heliophysical Year (IHY-2007) and now operates and continues to expand within International Space Weather Initiative (ISWI). SEVAN detectors measure time series of charged and neutral secondary particles born in cascades originating in the atmosphere by nuclear interactions of protons and nuclei accelerated in the Galaxy and nearby the sun. The SEVAN network is compatible with the currently operating high-latitude neutron monitor networks “Spaceship earth” (Kuwabara et al. 2006), coordinated by the Bartol Research Center, the Solar Neutron Telescopes (SNT) network coordinated by Nagoya University (Tsuchiya et

al. 2001), the Global Muon Detector Network (GMDN) (Munakata et al. 2000, Rockenbach et al., 2011), the Neutron Monitor Data Base (NMDB, Mavromichalaki et al. 2011, <http://www.nmdb.eu/>), International GLE database <http://gle.oulu.fi/> and a new muon–neutron telescope constructed at Yangbajing, Tibet, China (Zhang et al., 2010).

Three SEVAN modules are operating in Armenia (on the slopes of Aragats Mt.: 40.25N, 44.15E, altitude 2000, 3200 m and in Yerevan, altitude 1000 m), in Croatia (Zagreb observatory: 45.82N, 15.97E, altitude 120m), Bulgaria (Mt. Musala: 42.1N, 23.35E, altitude 2930 m), India (New-Delhi JNU Univ.: 28.61N, 77.23E, altitude 239 m) and in Slovakia (Mt. Lomnický Stit: 49.2N, 20.22E, altitude 2634 m). In fall 2017 SEVAN module was installed on Milesovka hill (50.6N, 13.9E, altitude 837 m) in Czech republic. The potential recipients of SEVAN modules are Italy, Israel, Germany and France. The analogical detector is in operation in China (Tibet: 30.11N, 90.53E, altitude 4300 m, Zhang et al., 2010).

The particle fluxes measured by the new network at medium to low latitudes, combined with information from satellites and particle detector networks at high latitudes will provide experimental evidence on the most energetic processes in the solar system and will constitute an important element of the global space weather monitoring and forecasting service. In this paper, we present the description of SEVAN modules, its capacity to measure charged and neutral fluxes; expected purities and efficiencies of secondary cosmic ray registration, as well as the first physical results of the SEVAN network coordinated operation. Also, we demonstrate the ability to measure the energy spectra of the solar protons, possibilities to distinguish between neutron- and proton-initiated GLEs, and some other important properties of hybrid particle detectors. A separate chapter is dedicated to registration of the Thunderstorm ground enhancements (TGEs), new high-energy phenomena in the atmosphere. SEVAN modules, operating at the slopes of Mt. Aragats in Armenia during recent years have detected many TGE events in the fluxes of electrons and gamma rays, proving the existence of the strong electric fields in the thunderclouds in which the relativistic run-away electrons create

avalanches in the thunderstorm atmospheres (Chilingarian et al., 2010, 2011). SEVAN detectors were calibrated by the gamma ray flux of the most powerful TGEs and furthermore, the time series of the high energy muons detected by SEVAN open possibility to estimate the electrical structure of the thunderclouds, the key parameter for creating models of both TGE and lightning occurrences.

In the appendix, we add the calculations of the barometric coefficients and diurnal variations for the SEVAN network

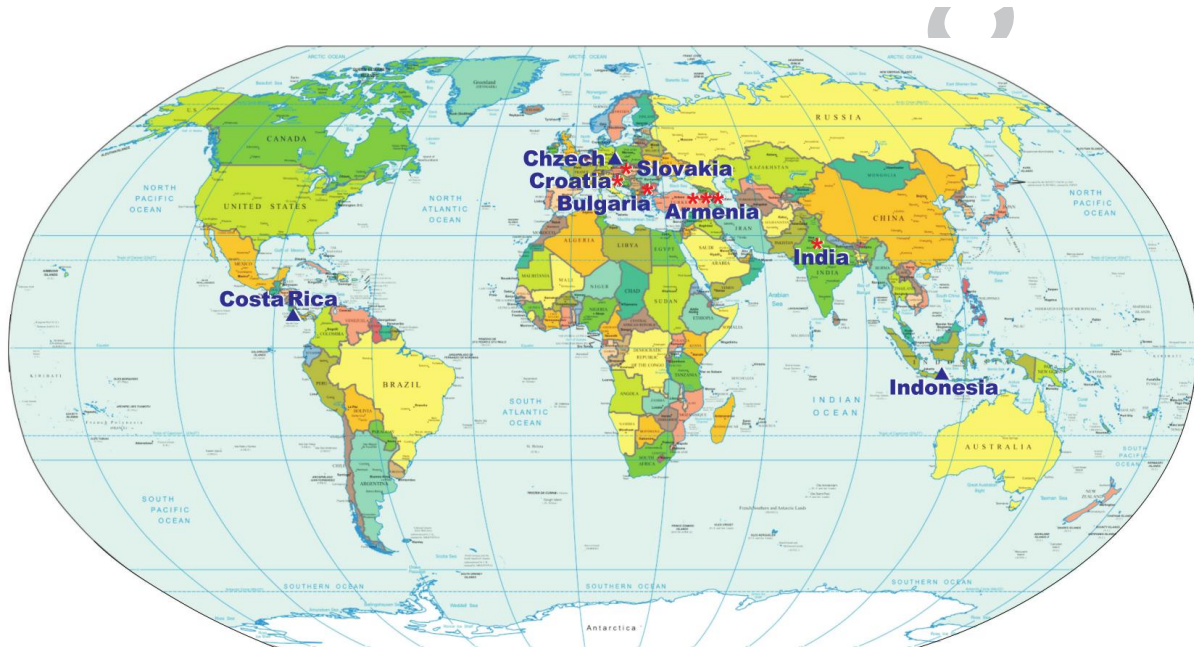


**Figure 1. SEVAN network: red asterisks – operating, blue triangles – planned locations.**

## 2. The basic module (unit) of the SEVAN network

Basic module of the SEVAN network (Fig. 2) is assembled from plastic scintillator slabs of  $50 \times 50 \times 5 \text{ cm}^3$  size. Between two identical assemblies of  $100 \times 100 \times 5 \text{ cm}^3$  scintillators (four standard slabs) two  $100 \times 100 \times 4.5 \text{ cm}^3$  lead absorbers and thick  $50 \times 50 \times 20 \text{ cm}^3$  scintillator stack (5 standard slabs) are located. Scintillator lights capture cones and Photomultipliers (PMTs) are located on the top, bottom and in the intermediate layers of the detector.

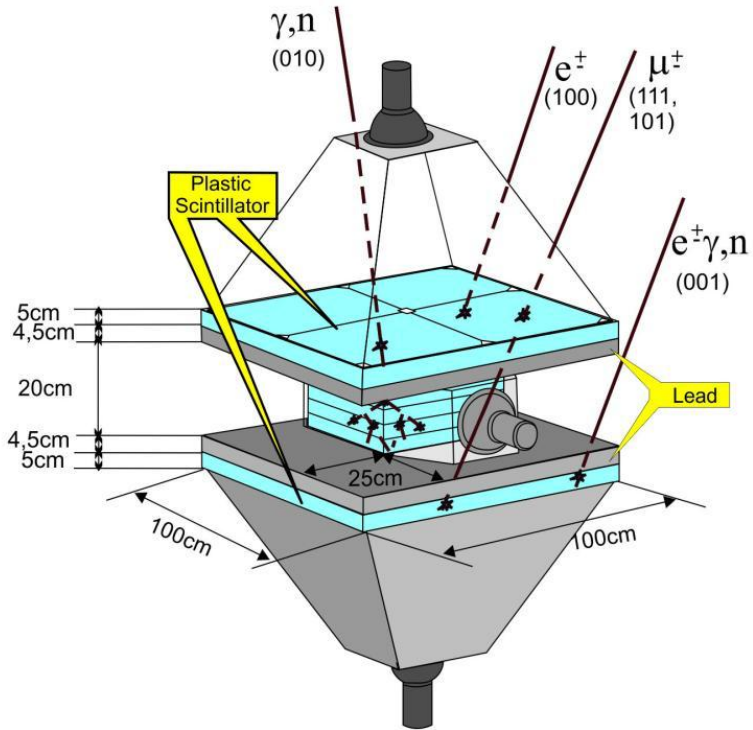


**Figure 2. SEVAN module measuring charged and neutral secondary cosmic rays**

Incoming neutral particles undergo nuclear reactions in the thick 20 cm plastic scintillator and produce charged particles. In the upper 5cm thick scintillator charged particles are registered very effectively; however, for the nuclear interactions of neutral particles there is not enough matter. When a neutral particle traverses the top thin (5cm) scintillator, usually no signal is produced. The absence of the signal in the upper scintillators, coinciding with the signal in the middle scintillator, indicates neutral particle traversal (gamma-ray or neutron). The coincidence of signals from the top and bottom scintillators indicates the traversal of high-energy muons. Microcontroller-based Data Acquisition (DAQ) electronics provides registration and storage of all logical combinations of the detector signals for further off-line analysis and for online alerts issuing. If we denote by “1” the signal from a scintillator and by “0” the absence of a signal, then the following combinations of the detector output are possible:

111 and 101—traversal of high energy muon; 010—traversal of a neutral particle; 100—traversal of a low energy charged particle stopped in the scintillator or in the first lead absorber. 110—traversal of a high energy charged particle stopped in the second lead absorber. 001—registration of inclined charged particles. The DAQ allows also the remote control of the PMT high voltage and of other important parameters of the detector. 10 years of operation prove high reliability of DAQ electronics. There no failures were noticed in the Eastern European SEVAN modules during operation period.

### **3. Characteristics of secondary cosmic ray fluxes detected by SEVAN modules**

The modules of the SEVAN network located on different latitudes, longitudes and altitudes are probing different populations of primary cosmic rays. The SEVAN modules measure fluxes of neutrons and gamma rays, of low energy charged particles and high-energy muons. To quantify statements on the detection of different types of particles by the SEVAN modules (efficiencies, purities of fluxes), we need to perform a detailed simulation of the detector response. We use simulated cascades of the charged and neutral secondary particles obtained with the CORSIKA (version 6.204) Monte Carlo code (Heck and Knapp, 1998). All secondary particles were tracked until their energy dropped below the predetermined value (50 MeV for hadrons, 10 MeV for muons and 6 MeV for electrons and gamma rays) or reached all the way to the ground level. The spectra of primary protons and helium nuclei (99% of the flux at energies up to 100 GeV) are selected to follow the proton and helium spectra reported by the CAPRICE98 balloon-borne experiment (Boezio et al., 2003). Among the different species of secondary particles, generated in nuclear- electromagnetic cascades in the atmosphere, muons, electrons,  $\gamma$ -rays, neutrons, protons, pions and kaons were followed by CORSIKA and stored. These particles were used as input for the GEANT3 package (GEANT, 1993), implemented for detector response simulation. Also, we take into account the light absorption in the scintillator (Chilingarian et al., 2007).

We show in Tab. 1 the most probable energies of primary protons to which the SEVAN modules are sensitive (Zazyan& Chilingarian, 2009). The calculations were made for different values of the

spectral index of the power law: for the GCRs ( $\gamma = -2.7$ ), columns 2-5; and for the SEP events ( $\gamma = -4, -5$ , and  $-6$ ), columns 6-9. Because in the simulations we use 3 values of SCR spectral indices we give an interval of energies of primary protons. From the Table, we can see that SEVAN network provides registration of the SEP events in a broad energy range including very poorly researched energies above 10 GeV. For instance, the neutron flux measured at Lomnisky Stit, Slovakia is sensitive to 4 GeV solar protons; and the high-energy muon flux measured at Delhi is sensitive to 18 GeV solar protons. Taking into account intermediate energies measured at Aragats, Armenia, Zagreb, Croatia and Musala, Bulgaria we can reliably recover SEP energy spectrum with satisfactory accuracy.

**Table 1. The range of the most probable energies (in GeV) of primary protons producing secondary fluxes at different SEVAN sites**

Station	GCR ( $\gamma=2.7$ )				SCR ( $\gamma=4,5,6$ )			
	Charged particles	Muons( $E > 250$ MeV)	Muons ( $E > 5$ GeV)	Neutron	Charge particles	Muons ( $E > 250$ MeV)	Muons ( $E > 5$ GeV)	Neutron
Yerevan (Armenia)	14.6	18.4	38.4	7.1	8.2–10.2	10–11.6	21.2 - 31.9	7.1
Nor-Amberd (Armenia)	13.1	14.9	41.2	7.1	7.6–10.6	9.7–11.3	20.5–31.3	7.1
Aragats (Armenia)	10.9	14.3	37	7.1	7.4–10	7.6–10.6	21.2–27	7.1
Musala (Bulgaria)	10.6	13.3	–	7.4	6.6–7.4	7.1–9.5	–	7.6–9.4
Zagreb (Croatia)	17.4	17.3	–	7.6	9.4–12.9	9.1–13.4	–	5.1–5.7
Lomnisky Stit (Slovakia)	11.5	14.5	–	4.1	4.1 –6.5	5.2–8.3	–	4
Delhi JNU (India)	18.1	18.1	–	16.5	14.2–15.1	14.3–15.3	–	14.3–14.4

The efficiency of the charged particle detection by all 3 layers of the SEVAN detector is above 95%; the neutron detection efficiency in the middle “thick” scintillator reaches 30% at 200 MeV, the efficiency of the gamma ray detection reaches 60% at the same energies. The purity (relative fraction of different species registered) of three SEVAN detecting layers is presented in Figure 3.

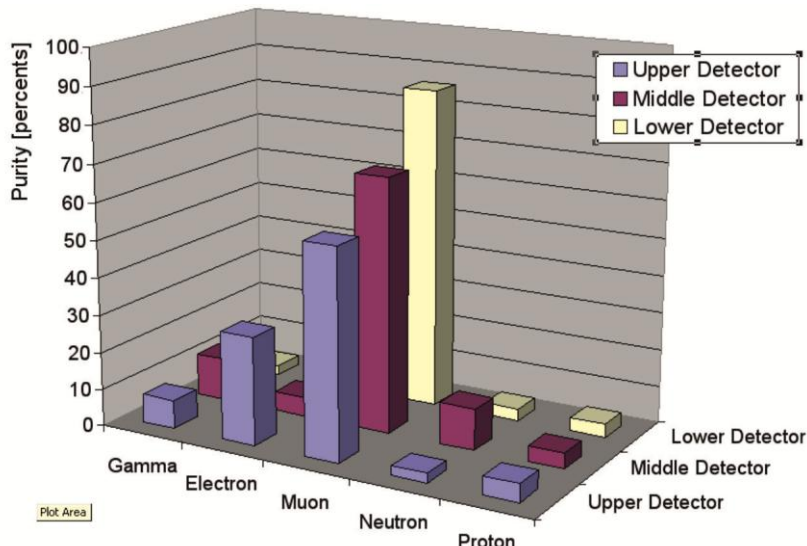


**Figure 3.The purity of the SEVAN detector layers.**

In Figure 3, we see that majority of registered particles in all three layers are muons; the first layer also registers electrons. The fraction of neutral particles is uppermost in the middle layer, although it is less than 10% there. It is apparent that using only layer counts we will not be able to research the modulation effects the sun poses on different species of secondary cosmic rays; we should “enrich” the detected fluxes by the particles of definite types. The coincidence techniques described in the previous section allow us to perform this task by registering different combinations of signals in the 3-layered detector. In Figure 4, we post the fraction of different particles registered by various combinations of the SEVAN module operation. The pattern is significantly improved: fraction of electrons selected by combination 100 is above 40%; the fraction of neutral particles selected by combination 010 – is larger than 85% and the fraction of high energy muons selected by combinations 111 and 101 reaches 95%. Therefore, by analyzing combinations, instead of layer counts, we can get clues how 3 types of secondary cosmic rays are influenced by meteorological and/or solar modulation effects. The data

from Figures 3 and 4 are tabulated in Table 2. The figures in the table show that coincidences of the detector layer can be used for selecting different particles of the secondary cosmic rays incident on the detector. For instance, ~81% of particles registered by combination 100 (signal only in the upper scintillator) are electrons and muons; ~86% of particles registered by combination 010 (signal only in the middle scintillator) are neutrons and gamma rays.

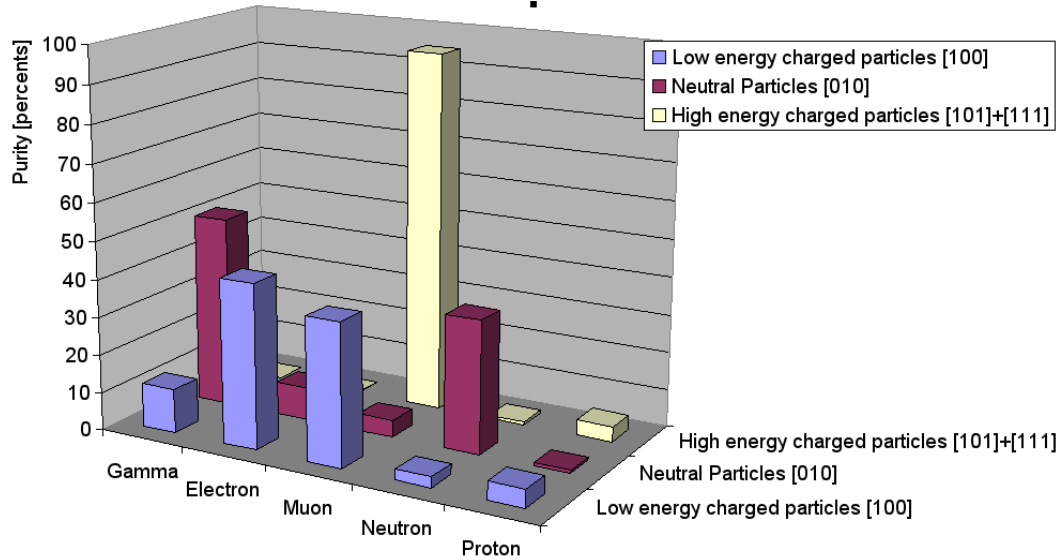


**Figure 4. Purity of SEVAN combinations.**

**Table 2. Summary of purity of selected particles by SEVAN layers and combinations.**

	Gamma %	Electron %	Muon %	Neutron %	Proton %
Low energy charged part. [100]	11.6	43.3	37.4	2.8	4.8
Neutral Particles [010]	50.6	8.8	4.4	35.1	1.0
High energy charged part. [101]+ [111]	0.0	0.11	94.9	0.81	4.1
Upper Detector	7.6	28.9	56.1	2.4	4.8
Middle Detector	11.6	5.2	67.9	11.0	4.2
Lower Detector	2.7	4.4	85.9	3.3	3.6

Of course, the purity is not the only parameter we are interested in; the efficiency of particle registration is also of the topmost interest in detector design and operation. In Figure 5, we post the

purity-efficiency diagram explaining which fraction of primary flux will contribute to different SEVAN combinations.

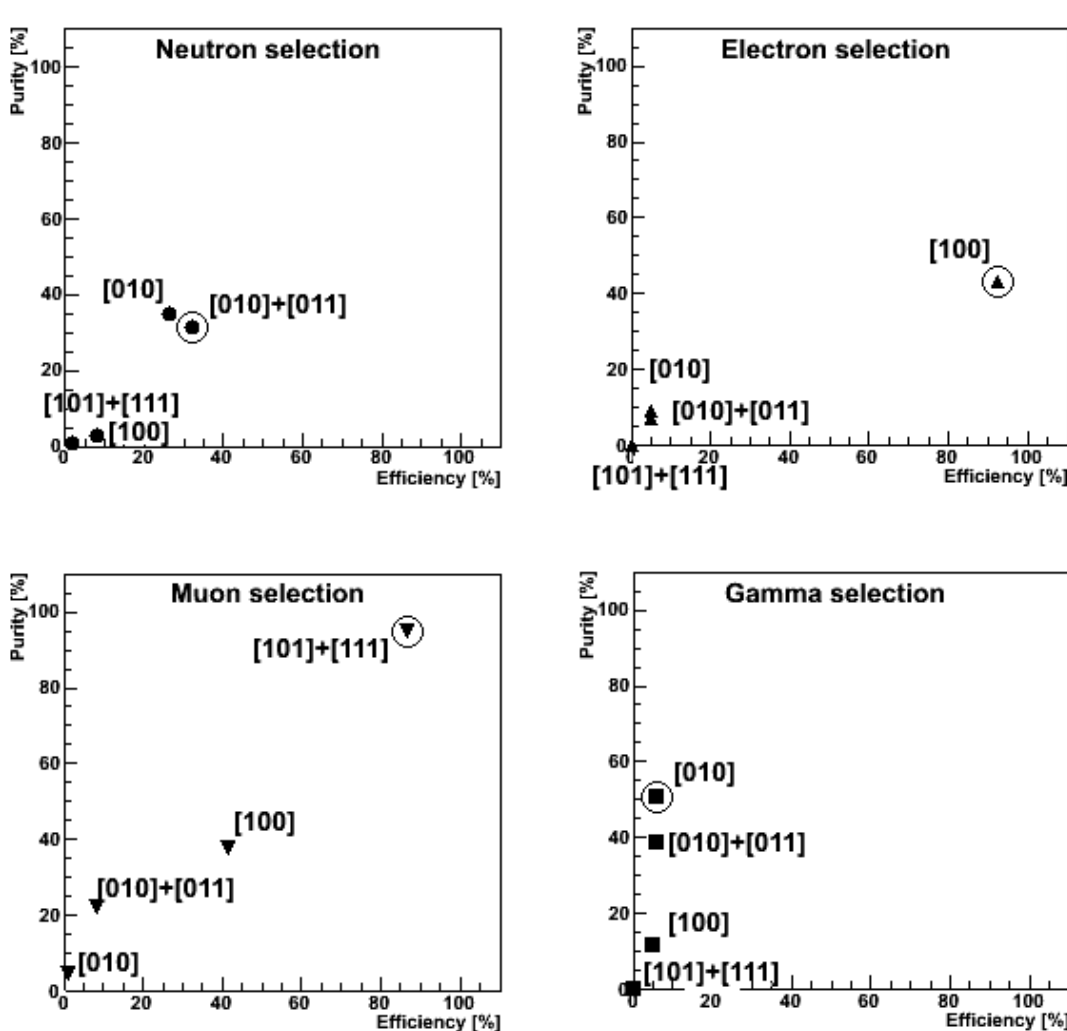


**Figure 5. The purity-efficiency diagram of the SEVAN combinations registering ambient population of the secondary cosmic rays generated by interactions of GCR with atmosphere.**

In Figure 5, we see that the high-energy muons are registered with both high efficiency and purity. Neutrons are registered with rather a satisfactory efficiency and purity (both ~30%). It is worth to mention that the efficiency of neutron monitor is reaching 30% only for highest energy neutrons. On the other hand, NM can distinguish neutrons from the gamma rays. Gamma rays are selected with lower efficiency by all possible combinations of SEVAN layers; nonetheless, efficiency of electron registration is above 90%; therefore, the low energy electromagnetic component is registered

efficiently by SEVAN. Moreover, combining SEVAN and NM measurements we can highly improve neutron-gamma ray discrimination.

In Table 3, we post the most probable energies (medians of the energy distribution of the parent protons) producing different elementary particles in the terrestrial atmosphere. Higher energy protons are responsible for the muon flux registered by SEVAN, lower energy primary protons can produce neutrons, registered by SEVAN.

**Table 3. Most probable energies of the GCRs registered by the SEVAN detector at 3200 m above sea level.**

Layers of detector located at 3200 m	Most probable energy of GCR (GeV)
Upper Layer	11.5
Middle 25 cm layer	8.5
Bottom Layer	14.5

As we can see, in Table 2 and in Fig. 5, SEVAN can register the low energy charged component, neutral component, and high-energy muons. In Table 4, we compare the simulated and measured one-minute count rates of these particles. Low energy charged particles, as well as neutrons and gamma rays, are attenuated very fast as they penetrate deep in the atmosphere. High-energy muons did not attenuate so fast as one can see in the last row of Table 4.

**Table 4. Experimental and simulated one-minute count rates measured by three scintillators of the SEVAN.**

	Yerevan (1000m)		NorAmberd (2000m)		Aragats (3200m)	
Type of Secondary particle	Measured count rate	simulated count rate	Measured count rate	simulated count rate	Measured count rate	simulated count rate
Low energy charged particles	8862±108	7202	11593±161	10220	16010±130	17330

<b>Neutral particles</b>	363±19	359	690±27	795	2007±46	1680
<b>High energy muon</b>	4337±67	5477	4473±99	5548	4056±64	8051

#### 4. Response of SEVAN particle detectors to GLEs initiated by the solar protons and neutrons

By observing solar neutrons, we can estimate the production time of the solar ions and also probe their energy spectrum. Thus, measurements of the time series of the solar neutrons will shed light on the operation of the solar accelerators. However, neutron events are very rare and it is not easy to distinguish them from more frequent proton events. The comparison of the count rate enhancements in the layers of the SEVAN module (measured in the number of standard deviations – “ $N\sigma$ ”) allows one to distinguish the GLE’s originated from solar neutrons incident on the terrestrial atmosphere. Table 5 shows that for neutron primaries there is a significant enhancement in the SEVAN thick layer and much less enhancement in a thin layer. For proton primaries the situation is vice-versa: the significant enhancement is in the thin layer, and much less in the thick layer.

**Table 5. Simulated enhancements (in standard deviations) of the “5-min” count rates corresponding to the GLEs initiated by primary neutrons, energy spectrum adopted from Watanabe et al, 2006) and primary protons (Energy spectrum adopted from Zazyan and Chilingarian, 2009).**

Detector layer	Solar Protons	Solar Neutrons
Upper 5 cm scintillator	4.8 $\sigma$	2.6 $\sigma$
Middle 20 cm scintillator	1.7 $\sigma$	6.4 $\sigma$

The one-minute count rate of the SEVAN upper layer (~25,500) is comparable to count rate of the Aragats standard 18NM64 type neutron monitor (~25,000), in spite the surface of SEVAN ( $1 \text{ m}^2$ ) is 18 times smaller than one of neutron monitor ( $18 \text{ m}^2$ ). The one-minute count rate of the SEVAN middle

layer ( $\sim 7700$ , surface  $0.25 \text{ m}^2$ ) is  $\sim 3.2$  times less than count rate of the Aragats standard 18NM64 type neutron monitor (25,000). However, most of neutron monitors of the worldwide network consists usually from only one section (6NM64). Thus, SEVAN provides approximately the same statistical significance in detecting neutral particles as 6NM64. Both low-energy charged particles registered by the upper layer and mostly neutral particles registered by the middle layer are sensitive to the modulation effects that solar activity pose on the intensity and directivity of the GCRs and these effects can be observed and researched by the SEVAN network. However, for the reliable registration of the differential energy spectra of very strong SEPs in the GeV region, we need particle detectors with the larger area and higher energy threshold. For instance, the most energetic particles from the GLE occurred on 20 January 2005 (energy of primary SEP  $\geq 20 \text{ GeV}$ ) were registered only by the  $100 \text{ m}^2$  array of underground muon detector of the GAMMA experiment (see details in Chilingarian, 2009). Of course, large magnetic spectrometer located on mountain altitudes will be a best solution for registration of highest energy solar cosmic rays. Unfortunately, the  $40 \text{ m}^2$  area and 3 TeV maximal detectable momentum magnetic spectrometer of ANI experiment (Danilova et al., 1982) planned in 80-ths by Yerevan Physics Institute and Lebedev Physical Institute was not finished due to collapse of Soviet Union.

## 5. Forbush decrease events detected by the SEVAN network in the 24-th solar activity cycle

The Solar Cycle 24, the weakest solar cycle in more than a century, the solar maximum of this cycle having peaked at 82 (smoothed Monthly value of the sunspot number) in **April, 2014**; the lowest of any cycle since 1928 when Solar Cycle 16 peaked at 78 (<http://www.swpc.noaa.gov/products/solar-cycle-progression>) in agreement with the Gleissberg cycle with the period 90 – 100 years (Brajsa et al., 2015). The number of SEP events was very low and only two of them has GLE components: 2012 May 17 Gopalswamy et al., 2013) and 2014 January 6 (sub-GLE, Thakur et al., 2014). GLE and sub-GLE events were primarily observed by the South Pole neutron monitors (the increase of  $\sim 2.5\%$ ) while a few other neutron monitors recorded smaller increases; the proton acceleration during GLE 71 and sub-GLE occurred up to rigidities  $R \sim 2.3\text{--}2.5 \text{ GV}$  (Kravtsova and Sdobnov, 2017). Aragats Neutron Monitors and SEVAN network detectors located on Aragats did not register these events due to large cutoff rigidity ( $R \geq 7.5 \text{ GV}$ ). The latest GLE 72 occurred on 10 September 2017 also were not

detected by Aragats Neutron Monitors and SEVAN modules. Only high-latitude neutron monitors detected count rate enhancements, follow for details: <http://www.nmdb.eu/?q=node/501>.

However, we detect several Forbush decreases by both SEVAN detectors and Neutron Monitors. In the middle of February 2011 the active region, AR 11158 produced 3 solar flares of class M6.6 (13 February, solar coordinates S19, W03), M2.2 (14 February, solar coordinates S20, W14) and strongest X2.2 (15 February, solar coordinates S19, W03S21, W18). All 3 flares were accompanied with CMEs headed to the earth's direction. The worldwide network of neutron monitors detects at 18 February sizeable Forbush decrease. The SEVAN network as well detects Forbush decrease by 3 monitors located in Armenia and by monitors located in Zagreb observatory (Croatia) and Mt. Musala (Bulgaria). The SEVAN module located in India did not register Forbush decrease due to large geomagnetic cutoff. In Fig. 6 we see that Forbush decrease is much more pronounced on the mountain altitudes (6 a and 6b) comparing with seal level (6c). Also, the recovery time of Aragats SEVAN is much longer compering with Musala SEVAN. In Fig. 7 we compare Forbush decrease registration by the neutron monitors and SEVAN detectors located on Aragats and in Nor Amberd research station on altitudes 3200 and 2000 m correspondingly. There is a good coherence of Forbush decrease detection by different type detectors; Nor Amberd SEVAN is less sensitive to disturbances of the geomagnetic storm due to its location under a large amount of matter; i.e. low energy neutrons, most sensible to Forbush decrease are attenuated in the concrete slabs above the detector.

ACCEPTED

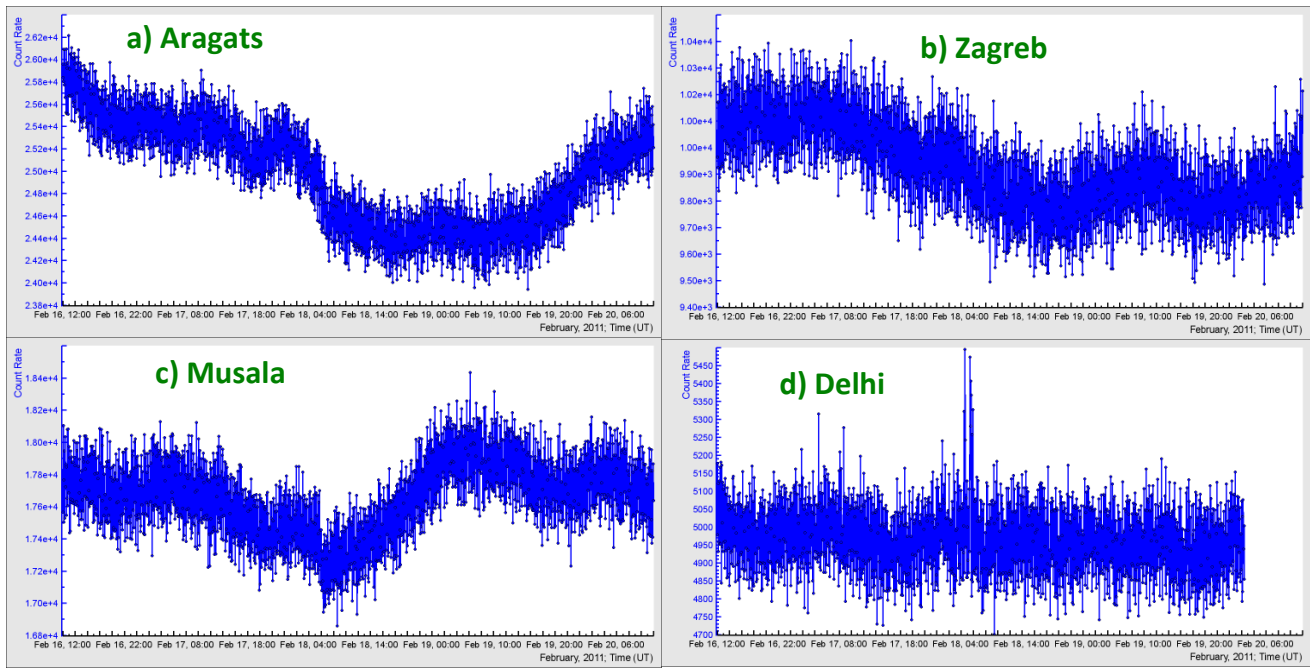


**Figure 6.** The time profiles of the FD on 18 February, 2011 measured by Aragats, Zagreb, Musala, and Delhi SEVAN monitors. The low energy charged particles (combination 100) time series.

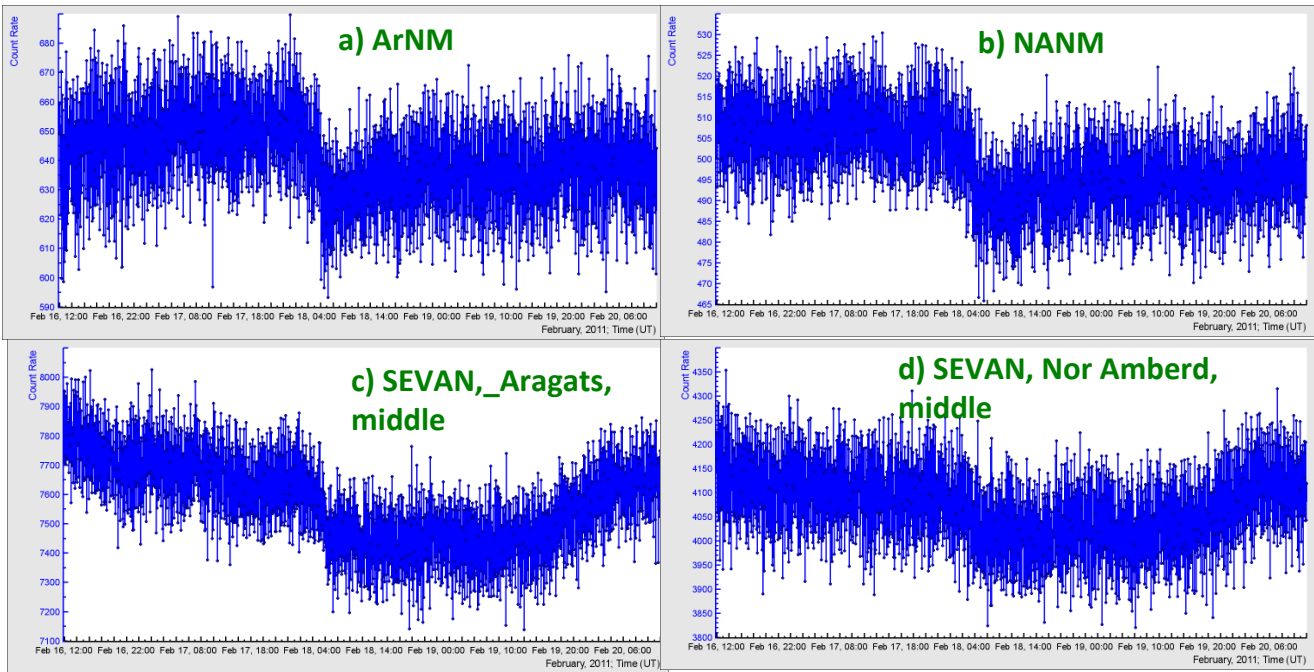


**Figure 7. Comparison of the FD detection by neutron monitors (from NMDB, normalized to 1 second count rate) and middle layer of SEVAN detector on Aragats and in Nor Amberg (1-minute count rate)**

The Forbush decrease phenomena is a global phenomena influenced whole globe (excepting the equatorial regions only where the cutoff rigidity is the largest); nevertheless, the detection of the local differences in time profiles of Forbush decreases produced by primary particles of different energies is very important and allows to recover the event anisotropy and sometimes also the shape of the ICME. The SEVAN network located at different longitudes (from Zagreb to Delhi) gives a possibility to explore the shape and the magnitude of the FD longitudinal dependence and its source (Belov et al., Ruffolo, 1999). In this respect, the registration of FDs also in low and high-energy charged particle fluxes can bring additional information for the developing of the ICME. The amplitude of FD is dependent on the disturbance of the interplanetary magnetic field caused by the ICME propagation and ICME interaction with the geomagnetic field. Both effects are dependent on the strength of the magnetic field “frozen” in the ICME (Chilingarian and Bostanjyan, 2010). GCRs are traversing the regions of the disturbed IMF and dependent on their energy are deflected from their path and miss encounter with earth atmosphere. As we demonstrate above different components of secondary cosmic rays detected on the earth surface are generated in the terrestrial atmosphere by interactions of CRs of

various energies; neutrons are generated by protons of lower energies than ones generating electrons; electrons, in turn, are generated by protons with energies lower than ones generated high energy muons. Therefore, the amplitudes of Forbush decrease in neutron, electron, and muon fluxes are expected to reflect these energy relations.

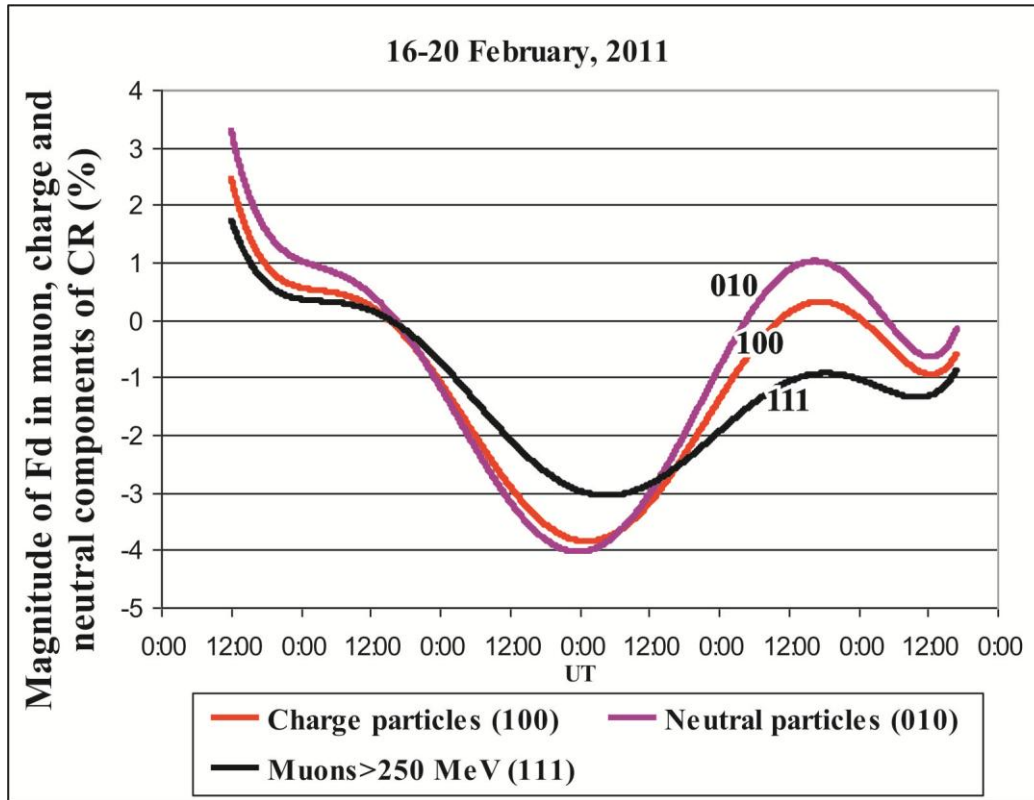


**Figure 8. FD as detected by different species of secondary cosmic rays (Aragats SEVAN detector combinations).**

In the Figure 8 and Table 6 we see that neutral component measured by Aragats SEVAN 010 combination demonstrate 4% decrease practically coinciding with FD measured by the Aragats neutron monitor (4.2%), the low energy charged component (100 combination) demonstrates ~3.8% decrease and the 111 combination (high energy muons) ~3% decrease. Nor Amberg SEVAN also demonstrated the biggest magnitude of FD for the neutral particles; however, the magnitude of the low energy charged particles (100) is a bit lower compared with the magnitude of FD measured in the high-energy muon flux. In Zagreb, magnitudes of Forbush decrease for all combinations were -3%.

**Table 6. The magnitudes of Forbush decrease (FD) measured by SEVAN network and Aragats**

neutron monitor on 18 February.

	Magnitude of FD Aragats, 3200m(%)	Magnitude of FD by Nor Amberd, 2000m (%)	Magnitude of FD by Zagreb 130m (%)	Magnitude of FD Musala 2900 m (%)	India, New Delhi JNU
SEVAN(100)	-3.8	-2.1	-3	-3	0
SEVAN(010)	-4	-4.2	-3	-	0
SEVAN(111)	-3	-2.3	-3	-	0
Aragats NM	-4.2	-4.0			

Another solar eruption from active region AR1402 on 23 Jan 2012 at 03:38 UT, produced an M8.7 flare is associated with full halo CME of 2000 km/s speed reached earth at 24 January; in Figure 9 and Table 7, we show FD detection by SEVAN network.

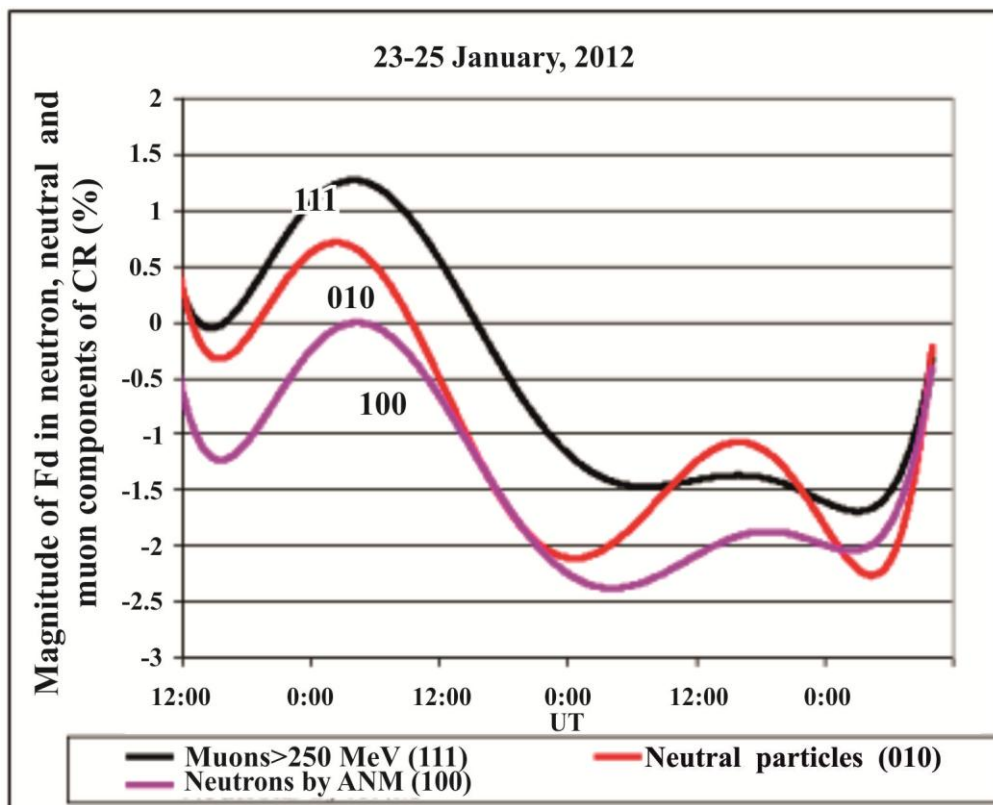


**Figure 9. FD of 24 January detected by the Aragats Neutron monitor and SEVAN (010) and 111 combinations.**

**Table 7. The magnitudes of FD measured by SEVAN network and Aragats neutron monitor on 24 January, 2012.**

	Magnitude of FD Aragats, 3200m (%)	Magnitude of FD by Nor Amberd, 2000m (%)
SEVAN(100)	-1.8	-2.1
SEVAN(010)	-2.1	-3
SEVAN(111)	-1.5	-2
Aragats NM	-2.4	-2.2

SEVAN network detects the Forbush decreases of 18 February 2011 and 24 January 2012 in the fluxes

of neutrons, low energy charged particles and high-energy muons. The patterns of Forbush decrease in different secondary particle species are very similar to ones measured by the NMIs only in atmospheric neutron fluxes. However, in addition to neutron monitors, SEVAN simultaneously measures FD patterns of other species of secondary cosmic rays giving additional clues for the recovering of the shape and frozen magnetic field of the ICME interacted with the magnetosphere.

## **6. Thunderstorm Ground Enhancements (TGE) detected by SEVAN and muon deficit**

Copious observations of the Thunderstorm ground Enhancements (TGEs, Chilingarian et al., 2010, 2011), i.e. enhanced fluxes of electrons, gamma rays and neutrons detected by particle detectors located on the earth's surface and related to the strong thunderstorms overhead, posed the question of their origin. According to the TGE initiation model (Chilingarian, 2014), the electric field of the lower dipole in the thundercloud effectively transfers the field energy to secondary cosmic ray electrons. Electrons by a Runaway Breakdown (RB, Gurevich et al., 1992) now referred as a Relativistic runaway electron avalanches (RREA, Babich et al., 1998, Dwyer, 2007, Khaerdinov et al., 2005) generate electron-gamma ray avalanches and gamma rays by photonuclear reaction create neutrons (Chilingarian et. al., 2012). TGEs occur during the extended periods of large negative electric fields measured at earth's surface (Chilingarian and Mkrtchyan, 2012). To produce large TGEs, clouds should be very close to the earth's surface (25-100 m) to allow electrons and gamma rays reach the particle detectors. Facilities of the Aragats Space Environment Center (ASEC, Chilingarian et al, 2005) observe charged and neutral fluxes of secondary cosmic rays by the variety of particle detectors located in Yerevan and on slopes of Mt. Aragats at altitudes 2000 and 3200 m. Observational data of the Aragats station's monitors obtained during 2008-2017 brings >500 TGE events allowing the detailed analyses and taxonomy of new high-energy phenomena in the atmosphere (HEPA). In Fig. 10 we show one of the largest TGE events observed by SEVAN detector. On October 4, 2010 a huge excess of low energy gamma rays and electrons was detected by the upper scintillator of SEVAN detector (combination 100) reaching  $60\sigma$  at 18:23! The energy threshold of the upper detector due the

matter of the roof above is  $\sim 7$  MeV. The peak in the time series of middle SEVAN scintillator located under 4.5 cm of lead is due to penetrated high-energy gamma rays of electron-gamma ray avalanche originated in the thundercloud. For the same minutes, the channels 111 (muons) shows pronounced decrease  $\sim -6\%$ . The energy of particles (mostly muons) necessary to penetrate lead filters and be detected in all three layers (combination 111) is  $\sim 250$  MeV.

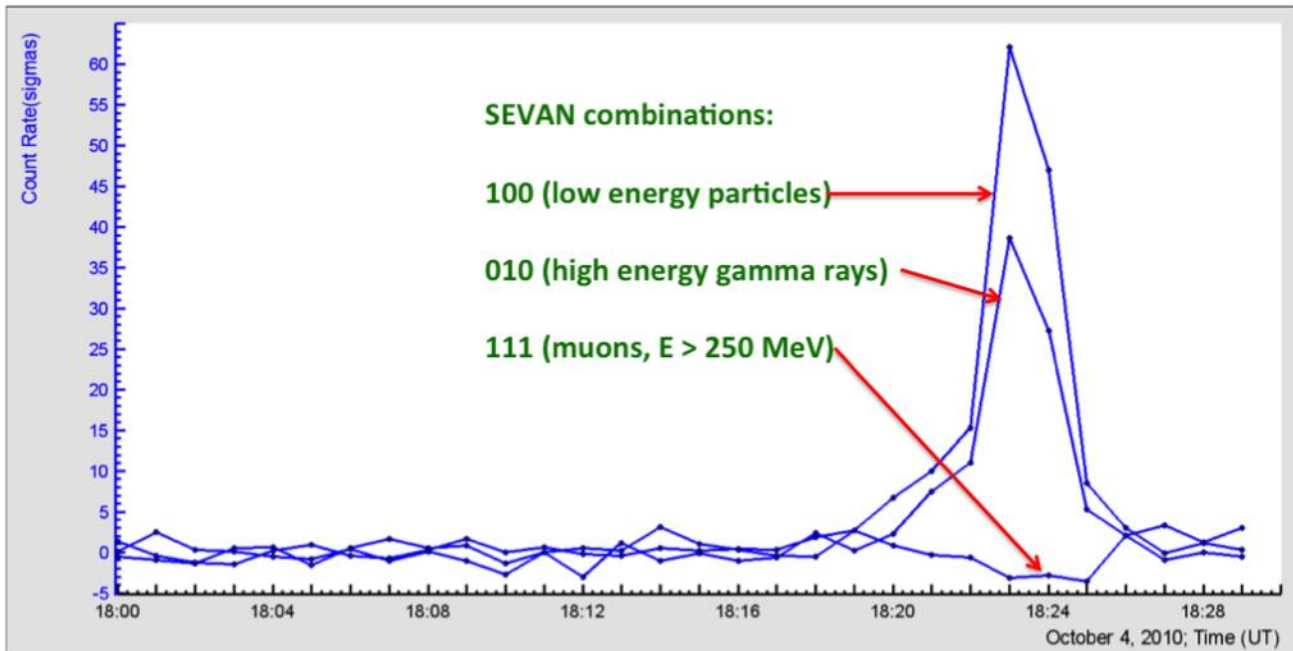


**Figure 10.** The count rates of SEVAN 100, 010, and 111 combinations in a number of standard deviations from the mean value measured at the fair weather before a thunderstorm. Huge TGE is detected in high-energy gamma ray flux (010) and low energy particle flux (100). Simultaneously deficit is detected in high-energy muon flux ( $>250$  MeV)

The huge flux of the gamma rays measure at 18:23 on 4 October 2010 was used to check the Aragats SEVAN ability to detect gamma ray flux by 010 the combination (signal only in the middle scintillator). The differential energy spectrum of the TGE event was recovered using energy-release histograms measured by the 60 cm thick plastic scintillators of the Aragats Solar Neutron Telescope (ASNT, see details in Chilingarian et.al., 2012). Using known energy spectrum and simulating the passage of the gamma-rays through the matter of roof and detector, and taking into account the detector response to gamma rays and electrons, we have estimated the expected number of gamma rays

detected by the “010” combination to be 1459 respectively. This value is in a good agreement with the experimentally measured value of  $1452 \pm 42$  (statistical errors only).

Observation of numerous TGEs by the Japanese, Chinese, Slovakian groups (Kuroda et al., 2016, Zeng et al., 2013, Wang et al., 2015, Torii et al., 2011, Tsuchiya et al., 2013, Kollarek et al., 2016) prove that RB/RREA is a robust and realistic mechanism for electron acceleration and multiplication leaving no doubts about correctness of the model of TGE initiation. Slovakian group detects TGEs with the SEVAN detector installed on Lomnický štít in 2014-207 (Kollarik et al., 2006, Kudela et al., 2017). Bulgarian group detected first TGEs as well on Musala Mt., the highest peak of Eastern Europe. Thus, SEVAN network becomes an important facility for the high-energy physics research in the atmosphere, as well as for the solar physics and space weather.

## 9. Conclusion

Reliable forecasts of major geomagnetic and radiation storms are of great importance because of associated Space Weather conditions leading to failures of space and ground-based technologies as well as posing radiation hazards on crew and passengers of satellites and aircraft. Measurements of Solar Wind parameters performed at spacecraft located at L1 provide too short time span for mitigation actions to be taken. Networks of particle detectors on earth’s surface provide timely information and constitute an important element of planetary Space Weather warning services. The big advantage of ground-based particle detectors is their consistency, 24 h coverage, multi-year operation and large area. In contrast, the planned life of the satellites and spacecraft is only a few years, they are affected by the same solar blast that they should alert, and space-born facilities instead of sending warnings are usually set in the standby mode during violent space storms.

The multi-layered detectors proposed in the present paper will probe different populations of primary cosmic rays. The basic detector of the SEVAN network is designed to measure fluxes of neutrons and gamma rays, of low energy charged particles and high-energy muons. The rich information obtained

from the SEVAN network will allow estimating the solar modulation effects posed on different species of GCRs and fluxes of charged and neutral particles from the highest energy SEP. To understand the sensitivity of the new type of particle detectors to high-energy solar ions we investigate the response of SEVAN modules to galactic and solar protons of highest energies. SEVAN network will be able to detect the hard spectra of solar ions (like 20 January 2005 GLE, Bostanjyan and Chilingaryan, 2007) preceded the upcoming very intense solar ion flux with rigidities  $>50$  MV dangerous for satellite electronics and astronauts. The SEVAN network detectors will also allow distinguishing very interesting GLEs initiated by the primary neutrons.

The network of hybrid particle detectors, measuring neutral and charged fluxes provide the following advantages over existing detector networks measuring single species of secondary cosmic rays (Neutron Monitors and Muon detectors):

- Measure count rates of the 3 species of the Secondary cosmic rays: charged particles with energy threshold 7 MeV, neutral particles (gamma rays and neutrons) and high-energy muons (above 250 MeV);
- Probe different populations of primary cosmic rays with rigidities up to GV;
- Reconstruct SEP spectra and determine position of the spectral “knees”;
- Classify GLEs initiated by solar protons and neutrons;
- Give possibilities to investigate energy dependences of the barometric coefficients and diurnal wave;
- Significantly enlarge the reliability of Space Weather alerts due to detection of three particle fluxes;
- Detect TGEs in high-energy gamma ray and low energy charged particle fluxes;
- Address one of the most important problems of the atmospheric physics – cloud electrification by measuring surge and deficit of detected particle fluxes;

- Research the runaway electron acceleration during thunderstorms and the enigma of lightning initiation;
- 10 years of operation prove high reliability of the SEVAN modules: there were no failures in the Eastern European SEVAN modules during whole operation period;
- Data Acquisition (DAQ) is Microcontroller-based provides registration and storage of all logical combinations of the detector signals and the remote control of the PMT high voltage and of other important parameters of the detector.  
m asl).
- SEVAN modules comprised from plastic scintillators are relatively cheap compared with ones using more expensive sensors, for instance  $^3\text{He}$  counters.

The phenomenon of decreasing of the high-energy muon flux measured by SEVAN detector during TGEs can be explained by the shifting of energetic spectra of muons in the electric fields inside cloud. During positive electric field in the lower dipole that accelerates electrons and negative muons downwards spectrum of negative muons shifts right, whereas spectrum of positive muons shifts left proportional to the net potential difference of the electric field. as a result of such a transformation, the fluxes of muons are changed: the flux of negative muons increases, while the flux of positive muons decreases. Thus, the total particle's flux decreases because the number of positive muons is greater (~30% at energies below 100 MeV) than the number of negative muons. By the measured deeps in high energy muon time series it is possible to remotely estimate the total potential drop in a thundercloud; the problem that escapes the solution till now because of the absence of adequate techniques for the measuring of the electric field inside thunderclouds. SEVAN modules installed on mountains Aragats, Lomnický štít , Musala and in Zagreb observatory are actively participating in the research in the new emerging field of high-energy physics in the atmosphere (HEPA). Thus, with one and the same detector, we can measure both the solar-terrestrial relations due to violent bursts on the sun and atmospheric high-energy physics activity due to strong atmospheric storms. Cheap and reliable

SEVAN detectors can be installed in other countries on different latitudes and longitudes to participate in the global network of monitoring Solar-terrestrial relations. Eastern European SEVAN network was expanded in 2017 by establishing SEVAN node at Milesovka hill in Czech republic ( $50^{\circ} 33' 18''$  N,  $13^{\circ} 55' 53''$  E, 837).

**Acknowledgements:** SEVAN network was developed in the framework of IHY-2007 initiative, and we thank H.Haubold, J.Davila, N. Gopalswamy for being so instrumental in helping us in this scientific endeavor. Authors thank K.Arakelyan and D.Pokhsraryan for commissioning the SEVAN units in India, Bulgaria, Croatia and Slovakia and A.Reymers for calculating SEVAN units' response function. Authors thanks SEVAN instrument hosts D. Rosa, N.Nikolova, K. Kudela, S. Mukherjee and O.Ploc for their interest to be a part of SEVAN network and for operating SEVAN modules. A.C. appreciates the support by Russian Science Foundation grant (project No. 17-12-01439). Time series from all nodes of SEVAN network are available from the WEB analysis platform ADEI:<http://www.crd.yerphi.am/adei>

### References:

- ACE News #87 – Feb 23, 2005. “Space Weather Aspects of the January 20, 2005 Solar Energetic Particle Event” [www.srl.caltech.edu/ACE/ACENews/ACENews87.html](http://www.srl.caltech.edu/ACE/ACENews/ACENews87.html)
- Asvestari E., Willamo T., Gil A., et al., 2017. Analysis of Ground Level Enhancements (GLE): Extreme solar energetic particle events have hard spectra, Advances in Space Research 60, 781–787.
- Babich L. P., Donskoi E. N., Kutsyk I. M., et al., 1998. Terrestrial gamma-ray flashes and neutron pulses from direct simulations of gigantic upward atmospheric discharge, Phys. Lett. A 245, 460.
- Belov A.V., Dorman L.I., Eroshenko E.A., et. al., 1995. Search for Predictors of Forbush Decreases., Proc. 24<sup>th</sup> Inter. Cosmic Ray Conf, 4, 888-891.
- Bostanjyan, N., Chilingaryan A., Eganov V., et al. , 2007. On the production of highest energy solar protons on 20 January 2005. Adv. Space res. 39, 1454-1457.
- Boezio M., Bonvicini V., Schiavon P., et al., 2003. The cosmic-ray proton and helium spectra measured with the CAPRICE98 balloon experiment, Astropart. Phys. 19, 583–604.
- Brajša G., Verbanac D., Sudar L., et al., 2015. A comparison between the observed and predicted amplitude of the 24th solar cycle r., Cent. Eur. Astrophys. Bull. 39, 1, 135–144.

Chapman S.(ed.), Annals of the International Geophysical Year, Pergamon Press, New York, vol. 1, 1959.

Chilingarian, A., Arakelyan, K., Avakyan, K., et al., 2005. Correlated measurements of secondary cosmic ray fluxes by the Aragats Space-Environmental Center monitors, Nucl. Instrum. Methods Phys. Res. Sect. A 543 (2–3) p.483–496.

Chilingarian A. and Reymers A., 2008. Investigations of the response of hybrid particle detectors for the Space Environmental Viewing and Analysis Network (SEVAN), Ann. Geophys, 26, (249- 257.

Chilingarian A., Bostanjyan N., 2010. On the relation of the Forbush decreases detected by ASEC monitors during the 23rd solar activity cycle with ICME parameters, Advances in Space Research 45, 614–621.

Chilingarian A., Hovsepyan G., Arakelyan K., et al., 2009. Space Environmental Viewing and Analysis Network (SEVAN), earth, Moon and Planets: Vol.104, Issue 1, 195.

Chilingarian A., 2009. Statistical study of the detection of solar protons of highest energies at 20 January 2005, Advances in Space Research 43 p. 702–707.

Chilingarian, A., and Bostanjyan N., 2009. Cosmic ray intensity increases detected by Aragats Space Environmental Center monitors during the 23rd solar activity cycle in correlation with geomagnetic storms, J. Geophys. Res., Vol. 114, No. A9, A09107.

Chilingarian, A. and Bostanjyan N., 2010. On the relation of the Forbush decreases detected by ASEC monitors during the 23rd solar activity cycle with ICME parameters, Advances in Space Research, 45, p. 614-621.

Chilingarian, A., Daryan A., Arakelyan K., et al., 2010. Ground-based observations of thunderstorm-correlated fluxes of high-energy electrons, gamma rays, and neutrons, Phys.Rev. D., 82, p. 043009.

Chilingarian, G. Hovsepyan, and A. Hovhannisyan, 2011. Particle bursts from thunderclouds: Natural particle accelerators above our heads, Physical review D 83, p. 062001.

Chilingarian, A. and Mkrtchyan, H., 2012. Role of the Lower Positive Charge Region (LPCR) in initiation of the Thunderstorm Ground Enhancements (TGEs), Physical Review D 86, 072003.

Chilingarian, A., Bostanjyan N., Karapetyan T., Vanyan L., 2012. Remarks on recent results on neutron production during thunderstorms, Physical Review D 86, 093017.

Chilingarian, B., Mailyan, Vanyan, L., 2012. Recovering of the energy spectra of electrons and gamma rays coming from the thunderclouds. *Atmos. Res.* 114–115, p. 1–16.

Chilingarian A., 2014. Thunderstorm Ground Enhancements – model and relation to lightning flashes, *J. Atmos. Solar-Terr. Phys.* 107, 68–76.

Chilingaryan S., Beglarian A., Kopmann A., et al., 2010. Advanced data extraction infrastructure: Web based system for management of time series data, *J. Phys. Conf. Ser.* 219, 042034.

Corti C., Bindi V., Consolandi C., et al., 2016. Solar modulation of the proton local interstellar spectrum with AMS-02, Voyager 1 and Pamela, *The Astrophysical Journal*, Volume 829, 8.

Danilova T., Dunaevsky A., Erlykin A. et al., 1982. Project of Hadron Interaction in the Energy Ranges  $10^3$  -  $10^5$  TeV Experiment (ANI Experiment), Proceedings of Academy of Science of Armenian Soviet Republic, physics series, Vol. 17, issue 3-4.

Dwyer J. R., 2007. Relativistic breakdown in planetary atmospheres, *Phys. Plasmas* 14, 042901.

Gopalswamy N, Xie H, Akiyama S, et al., 2013. The first ground level enhancement event of solar cycle 24: direct observation of shock formation and particle release heights, *Astrophys. J.*, 765, L30.

Gurevich A. V., Milikh G. M., and R. A. Roussel-Dupre, 1992. Runaway electron mechanism of air breakdown and preconditioning during a thunderstorm, *Phys. Lett. A* 165, 463.

Hatton C. J., 1971. Progress in Elementary Particles and Cosmic Ray Physics, 10, 1- 100, North Holland.

Heck D. and Knapp J., 1998. A Monte Carlo Code to Simulate Extensive Air Showers, Forschungszentrum, Karlsruhe, FZKA Report 6019.

Haurwitz M.W., Yoshida S. and Akasofu S.I., 1965. Interplanetary magnetic field asymmetries and their effects on polar cap absorption effects and Forbush decreases. *J. Geophys. Res.*, 70, 2977–2988.

Khaerdinov N. S., Lidvansky A. S., and Petkov V. B., 2005. Cosmic rays and the electric field of thunderclouds: Evidence for acceleration of particles (runaway electrons), *Atmos. Res.* 76, 346.

Kollárik M., Kudela K., Langer. R., et al., 2016. First results from the measuring equipment SEVAN on Lomnický štít: possible connections with atmospheric phenomena, Proceedings TEPA-2015, TIGRAN METS, 31-34, INSPIRE C15-10-02.

Kravtsova M.V. and Sdobnov V.E., 2017. Ground level enhancements of cosmic rays in solar cycle 24, *Astronomy Letters*, 43, 501.

Kudela K., Chum J., Kollárik M. et al., 2017. Correlations between secondary cosmic ray rates and strong electric fields at Lomnický Štít, *JGR Atmosphere, Journal of Geophysical Research: Atmospheres*, 122, 10,700–10,710.

Kuroda Y., S. Oguri S., Kato Y., et al., 2016. Observation of gamma ray bursts at ground level under the thunderclouds, *Physics Letters B* 758, 286–291.

Kuwabara, T., Bieber J. W., Clem J., et al. 2006. Realtime cosmic ray monitoring system for space weather, *Space Weather*, 4, S08001.

Labrador, A. W. and Cohen, C. M. S. and Cummings, et al., 2005. Solar-Particle Energy Spectra during the Large Events of October-November 2003 and January 2005, In: Proceedings of the 29th International Cosmic Ray Conference. Vol.1. Tata Institute of Fundamental Research , Pune, India, pp. 111-114.

Lantos, P., 2005. Radiation dozes potentially received on-board airplane during recent solar particle events, *Radiation Protection Dosimetry*, 118, 363-374.

Leerungnavarat K., Ruffolo D., Bieber J.W., 2003. Loss Cone Precursors to Forbush Decreases and Advance Warning of Space Weather Effects, *Astrophys. J.* 593 587–596.

Lockwood, J.A., Debrunner, H., Flukiger, E.O., and Ryan, J.M., 2002. Solar proton rigidity spectra from 1 to 10 GV of selected flare event since 1960, *Solar Physics*, 208 (1), 113-140.

Mavromichalaki, H., Papaioannou, A., Plainaki, C., et al., 2011. Applications and usage of the real-time neutron monitor database for solar particle events monitoring, *Adv. Space Res.* 47, 2210–2222.

Miroshnichenko L.I., *Solar Cosmic Rays: Fundamentals and Applications*, Second Edition, Springer, 2015.

Miroshnichenko L.I and Nymmik R.A., 2014. Extreme fluxes in solar energetic particle events: Methodological and physical limitations, *Radiation Measurements* 61, 6-15.

Munakata, K., J. W. Bieber, S. Yasue, et.al., 2000. Precursors of geomagnetic storms observed by the muon detector network, *J. Geophys.Res.*, 105(A12), 27,457–27,468.

Rockenbach M. , Dal Lago A., Gonzalez W. D., et.al., 2011. Geomagnetic storm's precursors observed from 2001 to 2007 with the Global Muon Detector Network (GMDN), *J. Geophys.Res.*, 38, L16108.

Roša D., Angelov Ch., Arakelyan K., et al., 2010. Seven CRO particle detector for solar physics and

space weather research, Cent. Eur. Astrophys. Bull. 34, 115–122.

Ruffolo D., Bieber J.W., Evenson P., et al. Precursors to Forbush Decreases and Space Weather Prediction ., Proceedings of the 26th International Cosmic Ray Conference. August 17- 25, 1999, Salt Lake City, Utah, USA.

Simpson J.A., 2000. The Cosmic Ray Nucleonic Component: the Invention and Science uses of the Neutron Monitor, Space Science Review 93, p. 11-32.

Shibata, S., 1994. Propagation of the solar neutron through the atmosphere of the earth, Journal of Geophysical Research, Vol. 99, NO. A4, 6651–6666.

Thakur N, Gopalswamy N, Xie H, et al., 2014. Ground level enhancement in the 2014 January 6 solar energetic particle event, *Astrophys. J.* 790 L13.

Thompson B.J., Gopalswamy N., Davila J.M., and Haubold H.J. (Eds.), Putting the “I” in IHY: The United Nations Report for the International Heliophysical Year 2007, Springer, Wien-New York, 2009.

Torii, T., Sugita, T., Kamogawa, M., et al., 2011. Migrating source of energetic radiation generated by thunderstorm activity. *Geophys. Res. Lett.* 38, L24801.

Tsuchiya H., Enoto T., Iwata K., et al., 2013. Hardening and termination of long-duration gamma rays detected prior to lightning, *Phys. Rev. Lett.* 111, 015001.

Wang X., Zhou X., Huang D., et al., 2015. Effects of the near-earth thunderstorms electric field on intensity of the ground cosmic ray electron at YBJ, PoS, ICRC2015, 233.

Watanabe, K., Gros, M., Stoker, P.H., et al., 2006. Solar neutron events of 2003 October–November, *Astrophysical Journal*, 636, 1135–1144.

Zazyan, M., Chilingarian, A., 2009. Calculations of the sensitivity of the particle detectors of ASECS and SEVAN networks to galactic and solar cosmic rays. *Astropart. Phys.* 32, 185–192.

Zeng Y., Zhu F.R., Jia H.Y., For the ARGO-YBJ collaboration, Correlation between cosmic ray flux and electric atmospheric field variations with the ARGO-YBJ experiment, 33ICRC, Rio de Janeiro, Brazil, 2013.

Zhang J.L., Tan Y.H., Wang H., et al., 2010. The Yangbajing Muon–Neutron Telescope, *NIMA*, 623, 1030-1034.

## Appendix

### 1. Calculation of the barometric coefficients for the SEVAN network

To recover and analyze the solar modulation of the Galactic Cosmic Rays (GCR) the influence of the meteorological effects on the flux of the secondary particles reaching the Earth surface should be carefully disentangled. Theory of meteorological effects (Dorman & Dorman, 2005) gives the detailed classification of the metrological effects; it mentioned the barometric one as major influencing particle fluxes. Therefore, it is the greatest importance to accurately measure the barometric coefficients to “unfold” the solar modulation effects. Besides this main goal, there exist several independent research problems connected with rigidity, height and solar cycle phase dependence of the barometric coefficient. All these dependences can be investigated by SEVAN network due to different altitudes, various cutoff rigidities and planned long-term operation. At the minimum of solar activity, the GCR flux is enriched by abundant low energy (below 10 GeV) particles, blown out from the solar system by the intense solar wind at years of the maximum of solar activity. Particle detectors located at high latitudes are sensitive to lower primary energies as compared with detectors located at middle-low latitudes, because of lower cutoff rigidity. Detectors located at high altitudes are sensitive to lower primary energies and register more secondary particles than sea level detectors. Detectors registering muons are sensitive to higher energies of primary particles compared with detectors measuring neutrons. Thus, the following relations between barometric coefficients of various particle detectors located in different places and measuring diverse species of secondary CR can be expected:

- Barometric coefficient absolute value for the same secondary particle flux is greater for detectors located at high latitudes as compared with low latitudes;
- Barometric coefficient absolute value for the same secondary particle flux should be greater at minimum of solar activity as compared with maximum;
- Barometric coefficient absolute value for the same secondary particle flux should be greater for high mountain altitudes as compared with lower locations;
- Barometric coefficient absolute value should be larger for neutrons as compared with muons;

- Barometric coefficient absolute value should be larger for low energy muons as compared with high energy muons;
- Barometric coefficient absolute value should be inversely proportional to zenith angle of incident particle flux;
- Barometric coefficient absolute values should be lower for the greater dead times of neutron monitor.

All the mentioned dependences were investigated and discovered during the last 50 years by the networks of neutron monitors and muon detectors (Shea & Smart, 2000). However, due to the peculiarities of detection techniques, scarce statistics, highly different local meteorological conditions, cycle-to-cycle variations of solar activity, the obtained results on the mentioned dependencies are yet more qualitative and additional investigations of the interrelations of barometric coefficients are needed. SEVAN provides an ideal platform for such researches. Data for calculation of barometric coefficients of SEVAN modules were selected in 2008, when there were higher than 15 mb continuous changes of atmospheric pressure during the day, and also there were no disturbances of the Interplanetary Magnetic Field (day variations do not exceed 1.5–2 nT). The values of the IMF were obtained from instrument SWEPAM, Advanced Composition Explorer (ACE) spacecraft ([http://www.srl.caltech.edu/ACE/ASC/level2/lvl2DATA\\_MAG.html](http://www.srl.caltech.edu/ACE/ASC/level2/lvl2DATA_MAG.html)). The least square method was used to obtain the regression coefficients. Large values of the correlation coefficient prove the correct selection of the reference data. In Table 1 we summarize the calculated barometric coefficients of SEVAN modules. In the columns accordingly are posted the altitude; cutoff rigidity; barometric coefficient; goodness of fit in the form of the correlation coefficient; count rate; relative error; “Poisson” estimate of relative error (standard deviation divides by average count rate).

**Table 1. Barometric coefficients, count rates and relative errors of SEVAN units.**

Monitor	Altitude (m)	RC (GV)	Barometric coefficient (%/ mb)	Correlatio n coefficien t	Count rate (min)	Relativ e error	$\frac{1}{\sqrt{N}}$
Aragats SEVAN upper detector	3200	7.1	$-0.466 \pm 0.018$	0.994	20768	0.005	0.0069
Aragats SEVAN middle detector	3200	7.1	$-0.406 \pm 0.012$	0.996	6573	0.011	0.0123
Aragats SEVAN lower detector	3200	7.1	$-0.361 \pm 0.016$	0.992	12481	0.008	0.0089
Nor Amberg SEVAN upper detector	2000	7.1	$-0.274 \pm 0.016$	0.975	9100	0.011	0.0105

Nor Ambedr SEVAN middle detector	2000	7.1	$-0.342 \pm 0.023$	0.969	3988	0.015	0.0158
Nor Ambedr SEVAN lower detector	2000	7.1	$-0.262 \pm 0.017$	0.973	5103	0.014	0.0141
Yerevan SEVAN upper detector	1000	7.1	$-0.251 \pm 7.85E-05$	0.994	14815	0.008	0.0082
Yerevan SEVAN middle detector	1000	7.1	$-0.238 \pm 0.014$	0.981	3414	0.016	0.0171
Yerevan SEVAN lower detector	1000	7.1	$-0.190 \pm 0.025$	0.903	9505	0.011	0.0102

The values posted in the last two columns should be very close to each other if the Poisson process can describe the particle arrival. Any small deviation manifested the correlation between detector channels; any large correlation – failures in electronics or data acquisition software (see for details Hovhannisyan and Chilingarian, 2011). In Table 1 and 2 we present barometric coefficients for SEVAN detectors combinations, selecting different species of secondary cosmic rays. Of course, we cannot measure “pure” flux of neutrons, due to the contamination of gamma- quanta, and muons. However, as we see from Table 2, events selected as “neutrons” (coincidences 010 and 011) demonstrate barometric coefficients approximately twice as events selected as muons.

**Table 2. Barometric coefficients, count rates and relative errors of SEVAN monitors for different coincidences.**

Monitor	Altitude (m)	Rc (GV)	Barometric Coeff. %/mb	Correlation Coefficient	Count rate [min]	Relative error	$\frac{1}{\sqrt{N}}$
Aragats SEVAN Low energy charged particles (Coincidence 100)	3200	7.1	$-0.5 \pm 0.018$	0.995	15389	0.007	0.0080
Aragats SEVAN High energy muons (Coincidence 111+ Coincidence 101)	3200	7.1	$-0.351 \pm 0.038$	0.96	3868	0.014	0.0161

Aragats SEVAN neutrons (Coincidence 010)	3200	7.1	-0.511±0.018	0.995	1959	0.019	0.0225
Nor Amberd SEVAN Low energy charged particles (Coincidence 100)	2000	7.1	-0.281±0.022	0.957	5941	0.013	0.0129
Nor Amberd SEVAN High energy muons (Coincidence 111+ Coincidence 101)	2000	7.1	-0.242±0.022	0.952	1988	0.026	0.0224
Nor Amberd SEVAN neutrons (Coincidence 010)	2000	7.1	-0.54±0.070	0.899	674	0.037	0.0385
Yerevan SEVAN Low energy charged particles (Coincidence 100)	1000	7.1	-0.3±0.014	0.987	9446	0.010	0.0102
Yerevan SEVAN High energy muons (Coincidence 111+ Coincidence 101)	1000	7.1	-0.149±0.035	0.765	4714	0.015	0.0145
Yerevan SEVAN neutrons (Coincidence 010)	1000	7.1	-0.4±0.039	0.943	425	0.048	0.0485

## 2. Investigation of diurnal variations of cosmic rays using SEVAN network

The diurnal variations are the result of complex phenomena involving IMF, magnetosphere and, in addition, dependent on the latitude, longitude and altitude of detector location on the Earth. The diurnal CR variations comprise an important tool for understanding basic physics of the heliosphere and the Earth's magnetosphere. Diurnal variations can be characterized by the amplitude (maximal value) measured in daily time series and by phase (time of the maximal amplitude). Different species of the secondary CR undergo different diurnal variations. It is obvious that more the most probable primary energy of the monitored CR species – less should be the amplitude of diurnal variation. Therefore, the third parameter, characterizing the diurnal variations at definite location and time, is so called upper limiting rigidity, i.e., the threshold rigidity not influenced by the solar, interplanetary and geomagnetic disturbances. The detailed investigation of the diurnal variations can comprise a basis of scientific data to be used in a wide context of solar-terrestrial connections (Mailyan and Chilingarian, 2010). In this section we present measurements of the phase, amplitude for the SEVAN monitors at the minimum of the solar activity year. This data will be used for physical analysis of SEVAN particle

detectors data as 24-th solar activity cycle proceeds.

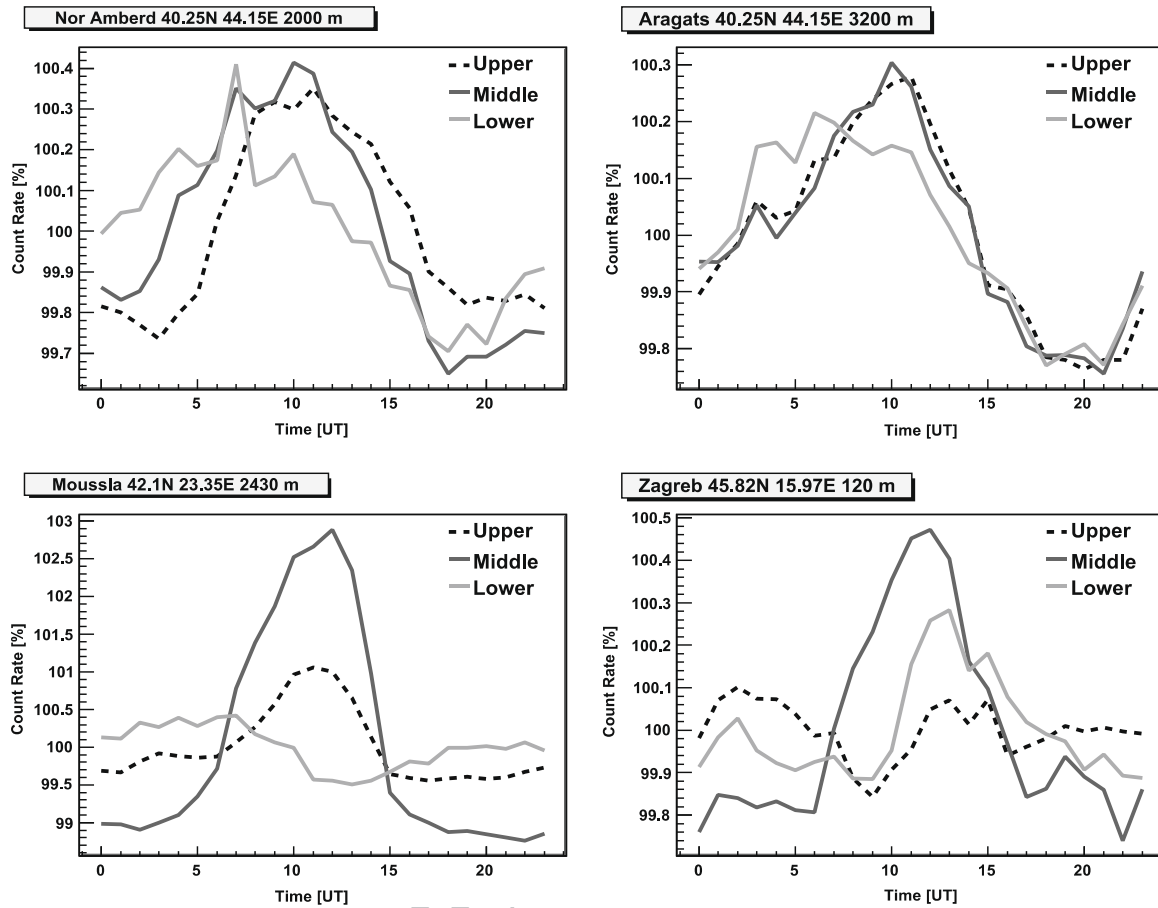


**Figure 11. Daily variations of high (lower layer) and low energy (upper layer) charged fluxes and neutral fluxes (middle layer) according to the SEVAN detectors located in Nor Amberd, Aragats, Musala and Zagreb. Month-averaged daily count rates of Nor Amberd May 2008 data, Aragats – October 2008, Musala and Zagreb December 2008–January 2009.**

In Fig. 11 we can see that detectors located at close geographic coordinates demonstrate similar patterns of the daily variations. When comparing Aragats, Croatian and Bulgarian monitors we can deduce that both latitude and longitude of site location influence the diurnal variations' pattern. However, the very large amplitude of Musala monitor's middle scintillator point on possible defects in light proofing of the middle detector. Filtered and pressure corrected (Chilingarian and Karapetyan, 2011) daily data from Figure 11 were fitted by the harmonic approximation function for each day of the selected period. In this way, distributions of amplitudes and phases of daily variation were got. The following approximation was used to be consistent with previous research (Kudela et al., 2008):

$$f(t_i) = A + B * \cos(\omega t_i + \psi) \quad (1)$$

Here  $A$  is the daily average value of cosmic ray intensity,  $B$  is the amplitude of daily variations,  $\omega$  is the angular frequency and  $\psi$  is the phase of daily variations. The quality of fit  $d$ , the difference between experimental data and the fit is calculated according to Kudela et al. (2008):

$$d^2 = \sum_{i=1}^n d_i^2 = \sum_{i=1}^n [Y_i - f(t_i)]^2 \quad (2)$$

Amplitudes and phases obtained from Eq. (1), and fit quality calculated by Eq. (2) are presented in Table 3. We do not fit curves with two peaks and without an apparent peak. For Nor Amberg SEVAN daily changes are bigger for the middle layer (enriched by neutrons and gamma rays). For Aragats all layers show similar behavior. In local times the maximums are at 12:00-15:00 for the upper detectors, and a few hours earlier for the lower detector. Aragats' scintillators also show maximum with magnitude about 0.2% at ~12:00 LT.

**Table 3. Daily variations of the SEVAN data; Nor Amberg data of May 2008, Aragats data of October 2008, Musala and Zagreb data of December 2008–January 2009.**

	Median amplitude (%)	Median phase (local time)	Quality of the fit (d)	Most probable primary energies (GV)
Nor Amberg SEVAN upper detector	0.28	15:13	1.33	14.6
Nor Amberg SEVAN middle detector	0.34	12:55	1.15	7.1
Nor Amberg SEVAN lower detector	0.24	10:36	0.18	18.4
Aragats SEVAN upper detector	0.23	12:42	0.71	14.6
Aragats SEVAN middle detector	0.21	12:27	0.62	7.1
Aragats SEVAN lower detector	0.20	11:17	0.33	18.4
SEVAN Musala upper detector	0.55	11:58	2.31	
SEVAN Musala middle detector	1.80	12:33	8.16	

SEVAN Musala lower detector	No peaks			
SEVAN Zagreb upper detector	Two peaks			
SEVAN Zagreb middle detector	0.28	12:39	1.35	
SEVAN Zagreb lower detector	0.12	14:43	0.51	

The primary data available from SEVAN network demonstrate that charged component variations are comparable with neutron variation and that diurnal variations are sensitive to longitude of site location.

## References

- Chilingarian A., Karapetyan T., 2011. Calculation of the barometric coefficients at the start of the 24th solar activity cycle for particle detectors of Aragats Space Environmental Center, *Advances in Space Research* 47, 1140–1146.
- Dorman L. I. and Dorman I. V., 2005. Possible influence of cosmic rays on climate through thunderstorm clouds, *Advances in Space Research*, Volume 35, pp 476-483.
- Hatton, C. J., 'The Neutron Monitor', in J. G. Wilson and S. A. Wouthuysen (eds.), *Progress in Elementary Particle and Cosmic Ray Physics X*, North Holland Publishing Co., Amsterdam, 1971.
- Hovhannisyan A., Chilingarian A., 2011. Median Filtering Algorithms for Multichannel Detectors, *Advances in Space Research*, 47(9), 1554-1557.
- Kudela, K., Firoz, K.A., Langer, R., et al., On diurnal variation of cosmic rays: statistical study of neutron monitor data including LominskyŠtit, in: Proc. 21st ECRS, 2008, s 4.15, p. 371-375, Kosice, Slovakia (available from link: <http://ecrs2008.saske.sk/dvd/s4.15.pdf>
- Mailyan B., Chilingarian A., 2010. Investigation of diurnal variations of cosmic ray fluxes measured with using ASEC and NMDB monitors, *Advances in Space Research* 45, 1380–1387.
- Shea & Smart, 2000. Fifty years of cosmic radiation data, *SSR*, 93, p. 229-262.